Journal of Power Sources 377 (2018) 87–92

Contents lists available at ScienceDirect

Journal of Power Sources

journal homepage: www.elsevier.com/locate/jpowsour

Short communication

LiCl-LiI molten salt electrolyte with bismuth-lead positive electrode for liquid metal battery

Junsoo Kim[a,1], Donghyeok Shin[b,1], Youngjae Jung[a], Soo Min Hwang[a], Taeseup Song[b,*], Youngsik Kim[a,**], Ungyu Paik[b,***]

[a] School of Energy and Chemical Engineering, Ulsan National Institute of Science and Technology (UNIST), UNIST-gil 50, Ulsan 44919, Republic of Korea
[b] Department of Energy Engineering, Hanyang University, Seoul 04763, Republic of Korea

HIGHLIGHTS

- Electrochemical behavior of the material was investigated for liquid metal cells.
- Low operation temperature was achieved by the eutectic composition of LiCl-LiI.
- The wetting behavior of Bi-Pb alloy was studied on the current collector substrate.
- Li|LiCl-LiI|Bi-Pb cells showed long cycle, high efficiency, and high rate capability.

GRAPHICAL ABSTRACT

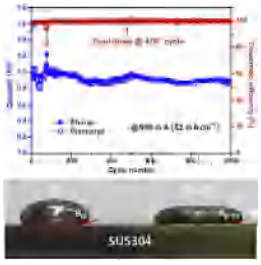

ARTICLE INFO

Keywords:
Molten salt
Alloy
Wettability
Liquid metal
Batteries

ABSTRACT

Liquid metal batteries (LMBs) are attractive energy storage device for large-scale energy storage system (ESS) due to the simple cell configuration and their high rate capability. The high operation temperature caused by high melting temperature of both the molten salt electrolyte and metal electrodes can induce the critical issues related to the maintenance cost and degradation of electrochemical properties resulting from the thermal corrosion of materials. Here, we report a new chemistry of LiCl-LiI electrolyte and Bi-Pb positive electrode to lower the operation temperature of Li-based LMBs and achieve the long-term stability. The cell (Li|LiCl-LiI|Bi-Pb) is operated at 410 °C by employing the LiCl-LiI (LiCl:LiI = 36:64 mol %) electrolyte and Bi-Pb alloy (Bi:Pb = 55.5:44.5 mol %) positive electrode. The cell shows excellent capacity retention (86.5%) and high Coulombic efficiencies over 99.3% at a high current density of 52 mA cm^{-2} during 1000^{th} cycles.

1. Introduction

The development of large-scale energy storage system (ESS) with low cost and long-term durability is crucial for the utilization of practical applications. Different types of ESSs have been suggested [1,2], but, electrochemical energy storage devices have been received significant attention for the application in ESS as they are free from the topographic requirement for the installation and simple for scaling up to MW levels [2–6]. Recently, Sadoway et al. developed liquid metal batteries (LMBs) aiming at the large-scale [7].

LMBs simply consist of liquid metals and molten salt as the negative and positive electrodes and electrolyte, respectively, which are

* Corresponding author.
** Corresponding author.
*** Corresponding author.
E-mail addresses: tssong@hanyang.ac.kr (T. Song), ykim@unist.ac.kr (Y. Kim), upaik@hanyang.ac.kr (U. Paik).
[1] Both authors contributed equally to this work.

https://doi.org/10.1016/j.jpowsour.2017.11.081
Received 25 August 2017; Received in revised form 1 November 2017; Accepted 26 November 2017

spontaneously divided into three distinct layers in liquid phase due to their thermodynamic immiscibility and difference in density [7]. Since the LMBs are operated in the liquid state, they have the advantages over typical batteries based on solid-state electrodes like: (1) no dendrite formation, (2) no phase deformation during cycling and (3) stable electrode/electrolyte interface, which enables safe operation and robust cycle performance [8]. Especially, the facile ion diffusion at the interface between liquids and high electronic conductivity facilitate the high rate capability suitable for ESS application involving fast charging and discharging.

The physicochemical properties of the molten salt electrolyte play an important role on the performance of the LMBs. There are five critical requirements for the molten salt electrolyte; (1) appropriate density between those of the positive and negative electrode, (2) no spontaneous side reaction with the electrode material, (3) minimal solubility of the liquid metal, (4) low melting temperature and (5) high ionic conductivity [7]. Li based halide salts have been employed as the electrolyte in LMBs with Li metal electrode: (1) LiCl-LiF (30:70 mol %) [9] (2) LiF-LiCl-LiBr (22:31:47 mol %) [10] and (3) LiF-LiCl-LiI (20:50:30 mol %) [11], which were operated at 550 °C, 500 °C and 450 °C, respectively. Because melting temperature of electrolyte usually determines the operation temperature of the cell, even multi-components with polyatomic anion salt and halide salt have been explored to reduce melting temperature [12].

Bi and Sb are good candidates as a positive electrode metal for LMB due to their high electronegativity. Despite the slightly lower voltage of Bi (0.75 V vs. Li/Li^+) compared to that of Sb (0.9 V vs. Li/Li^+), Bi is still attractive candidate owing to its low melting temperature of 271.3 °C, which could significantly reduce the operation temperature of LMB [13]. Based on electromotive force (EMF) measurements, Weppner and Huggins has reported that Li-Bi system has open circuit voltages (OCVs) ranging from 0.95 to 0.72 V (vs. Li/Li^+) depending on the Li concentration in Bi (0–75 mol %) [13]. Ning et al. demonstrated excellent electrochemical properties from Li|LiCl–LiF|Bi cell operating at 550 °C [9]. Since the cell operation temperature typically depends on the melting temperature of electrolytes due to its high melting temperature, developing electrolytes with a low melting temperature is significant to minimize the maintenance cost and corrosion of cell components toward practical applications of LMBs.

Here, we report a new composition of molten salt electrolyte and positive electrode to lower the operation temperature of Li-based LMBs. The eutectic composition of LiCl-LiI molten salt electrolyte (LiCl:LiI = 36:64 mol %, T_m = 368.2 °C) and Bi-Pb eutectic alloy (Bi:Pb = 55.5:44.5 mol %) have been employed as the electrolyte and positive electrode material to reduce the cell operation temperature to 410 °C. Also, the Bi-Pb eutectic alloy exhibits good wettability on the SUS 304 current collector. The Li|LiCl-LiI|Bi-Pb cell with 1 Ah capacity shows excellent cycle performance with capacity retention of 86.5% and high Coulombic efficiencies over 99.3% over 1000th cycles at a high current density of 52 mA cm^{-2}.

2. Experimental

Cell assembly and customized facilities: Figure S1 shows schematic illustration of cell assembly. The negative electrode was prepared by soaking Ni-Fe foam in the liquid Li. Alumina tube and ceramic sealant were used for electrical insulating and sealing, respectively (Figure S1a) [9]. All cell components are made by SUS304 because of its high corrosion resistance, heat resistance and machinability. High purity LiCl and LiI salts (99.9 and 99.95%, Alfa Aesar) were used for electrolyte and salts mixture (LiCl: LiI = 36:64 mol %) were ground, mixed, and melted in quartz tube. It was dried under vacuum by two steps (80 °C, 12 h/260 °C, 12 h) to remove residual water and subsequently melted under vacuum at 500 °C for 5 h (Figure S1b). Bulk Bi-Pb eutectic alloy (99.9%, Alfa Aesar, Bi:Pb = 55.5:44.5 wt %) was used for positive electrode material (Figure S1c). Positive electrode materials were placed in the bottom of the container followed by the addition of molten salt electrolyte considering the volume of the liquid state and the cap with Li filled Ni-Fe foam was joined to the cup (Figure S2, Table S1). The whole assembly processes were conducted in the Ar-filled glove box. The assembled cell was loaded in custom-built quartz vessel (Figure S3a) and heated up to operation temperature in customized vertical furnace under Ar atmosphere (Figure S3b).

Electrochemical tests and characterization: Galvanostatic charge/discharge experiments were carried out using cycler (WBCS 3000, Wonatech). The Leakage current was quantitatively determined by using stepped-potential measurements (ZIVE SP2, Wonatech). The melting temperature was analyzed by differential scanning calorimetry (DSC, Q200 SDT, sapphire as reference) heating from 50 °C ~ 550 °C at 10 °C/min under N_2 condition to prevent oxidizing the materials during the measurement. Before the DSC analysis, the LiCl-LiI mixture was carefully stored in the glove box to avoid the contact with air. The microstructure and elemental distribution were investigated by scanning electron microscopy (SEM) and energy dispersive X-ray spectroscopy (EDS). The phase identification was conducted by X-ray diffraction (XRD) with a Cu Kα X-ray. The electrochemical impedance spectroscopy was performed with the potentiostat (ZIVE SP2, Wonatech) in a frequency range of 10^4 to 100 Hz with amplitude of 10 mV.

3. Results and discussion

To lower the operation temperature of the LMBs, the salt mixture of the LiCl-LiI eutectic point (LiCl-LiI = 36:64 mol %, T_m = 368.2 °C) was designed by molten salt electrolyte in Li based halide salts based on its phase diagram (Figure S4a) [9–11,14]. Fig. 1a shows the DSC results of LiCl-LiI mixture before and after cycle, also the positive electrode material (Figure S4b). The LiCl-LiI mixture exhibits one strong endothermic reaction peak around 372 °C corresponding to the melting temperature (Fig. 1a). This result clearly shows the new molten salt electrolyte (LiCl-LiI = 36:64 mol %) has a lower melting temperature compared to that of the molten salt electrolytes employed in previous studies (LiCl-LiF = 30:70 mol %, T_m = 501 °C) [9], (LiF-LiCl-LiBr = 22:31:47 mol %, T_m = 430 °C) [10], (LiF-LiCl-LiI = 20:50:30 mol %, T_m = 430 °C) [11]. The blue line in Fig. 1a shows the DSC analysis result of LiCl-LiI mixture exposed to air (N_2: 70%, O_2: 30%). Three new endothermic peaks appear at 67, 78 and 128 °C as undesirable side reactions indicating high sensitivity of lithium halides to the oxygen. However, the new molten salt electrolyte after 500th cycles also shows one strong endothermic reaction peak at 373 °C without any side reactions. This result demonstrates that the electrolyte of LiCl-LiI has compatibility and stability with the Bi-Pb. Further evaluation of electrolyte was performed by stepped-potential measurement. The Li|LiCl-LiI|Bi-Pb cell indicates low leakage currents (< 0.05 mA/cm^2) when held at 1.1 V (Fig. 1b) which is below the previous study (1.0 mA/cm^2) [15]. The above results clearly demonstrate that the synthesized molten salt is a suitable electrolyte to suppress the self-discharging during cell operation.

Although low operation temperature of LMBs has several advantages in terms of maintenance cost and long-term stability resulting from suppression of thermal corrosion [16–19], it reduces the wettability of the liquid metal due to increase in surface tension of the liquid metal [20–22]. Low wettability of the positive electrode can increase the resistance at the interface with current collector by decreasing the interface area with electrolyte [23]. Furthermore, low wettability of the positive electrode decreases the gap between the negative and positive electrodes related with the cell safety issue caused by a short–circuit. We employed the Bi-Pb eutectic alloy as positive electrode to improve the wettability and kinetic associated with ion. The melting temperature of Bi-Pb eutectic alloy is 125.5 °C which is much lower than melting temperatures of each metal (T_m/Bi = 271.4 °C, T_m/Pb = 327.5 °C) [24]. Fig. 2a shows the wetting behavior of liquid Bi

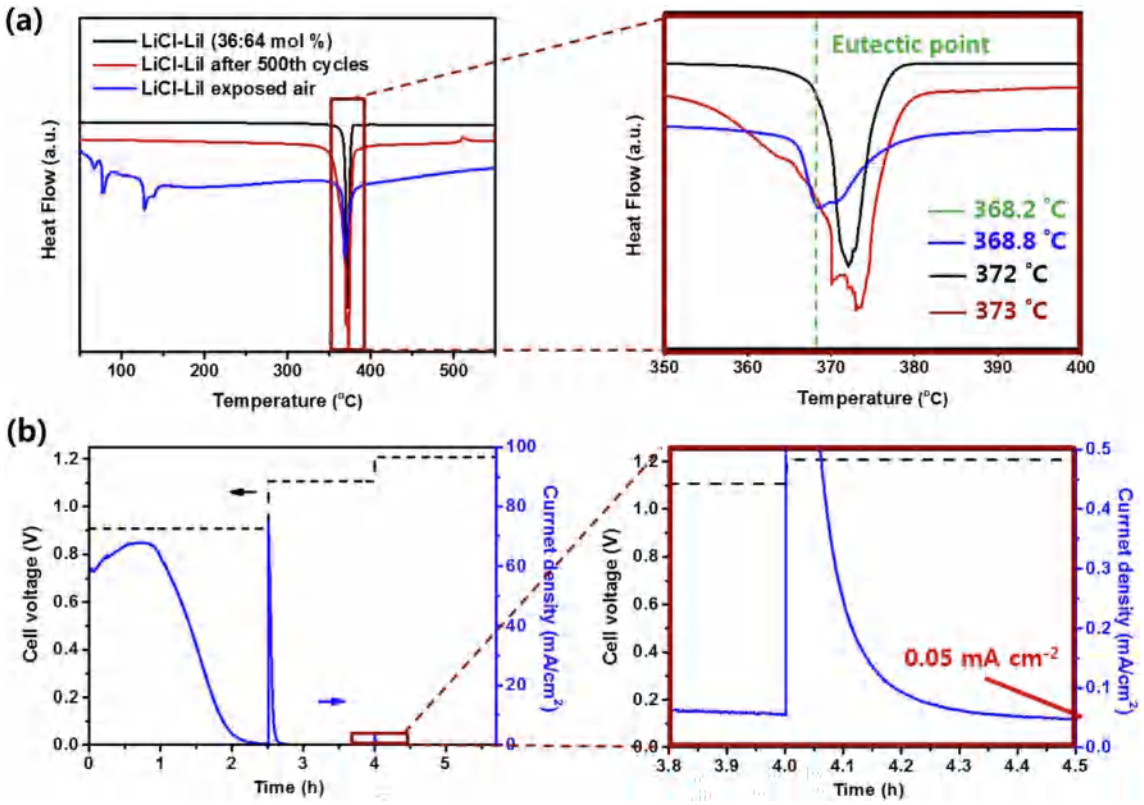

Fig. 1. (a) DSC analysis of LiCl-LiI electrolyte at different cycle and atmosphere: black (bare, under Ar); red (after 500th cycles, under Ar); blue (bare, exposed air consists of 70% N_2, 30% O_2). (b) Stepped potential measurement of Li|LiCl-LiI|Bi-Pb cell at 410 °C. (For interpretation of the references to colour in this figure legend, the reader is referred to the web version of this article.)

and Bi-Pb eutectic alloy on the SUS 304 substrate at 390 °C in Ar atmosphere. Bi was shown as more sphere shape than Bi-Pb eutectic alloy suggesting the higher wettability between Bi-Pb eutectic alloy and SUS304 than Bi. The cells with the equal mass of positive electrode were assembled to observe the difference of wetting behavior between Bi and Bi-Pb eutectic alloy in practical LMB cell. Fig. 2b shows the cross-sectional images of LMB cells with the Bi (left picture in Fig. 2b) and Bi-Pb eutectic alloy (right picture in Fig. 2b) as the positive electrode at the state of full discharge. Since the wetting behavior is significantly different, the heights of the Bi and Bi-Pb eutectic alloy from the current collector are shown that 0.37 cm and 0.25 cm, respectively (Figure S5). Thus, the use of Bi-Pb eutectic alloy not only reduces the cell operation temperature, but also addresses the safety issue.

Fig. 3a shows the cross-sectional image of Li|LiCl-LiI|Bi-Pb cells after removing the Li negative electrode at full discharge state. Three distinct layers corresponding to the electrolyte in the top, intermetallic compound in the middle and Bi-Pb alloy in the bottom are clearly observed. The composition in the interface between the intermetallic compound and Bi-Pb alloy was characterized by EDS analysis (Fig. 3b). During the sample preparation, Li compound is fully oxidized with H_2O in room temperature unlike metal alloy. It is considered that the distribution of Li element could be indirectly analyzed by the content of

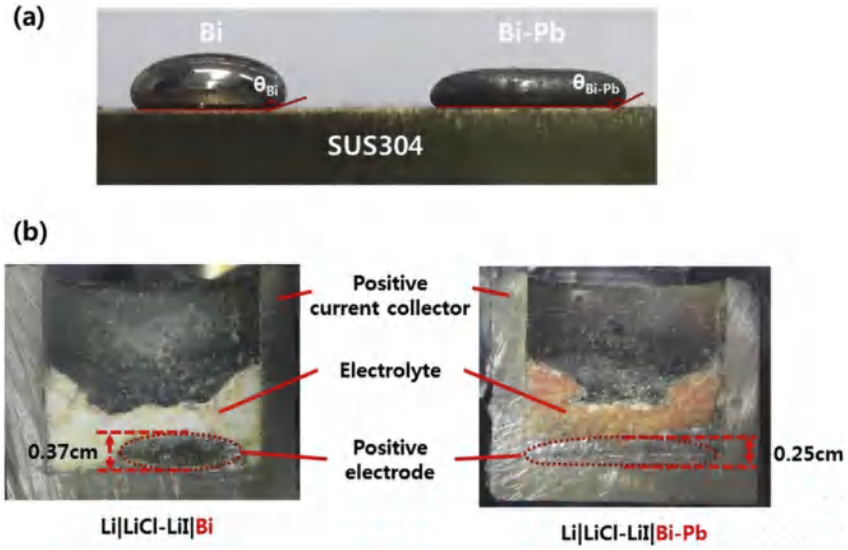

Fig. 2. (a) Photograph of liquid Bi and Bi-Pb eutectic alloy on SUS304 substrate and (b) Cross-section images of Li|LiCl-LiI|Bi cell (left) and Li|LiCl-LiI|Bi-Pb cell (right) at full charged state after cooling down to room temperature.

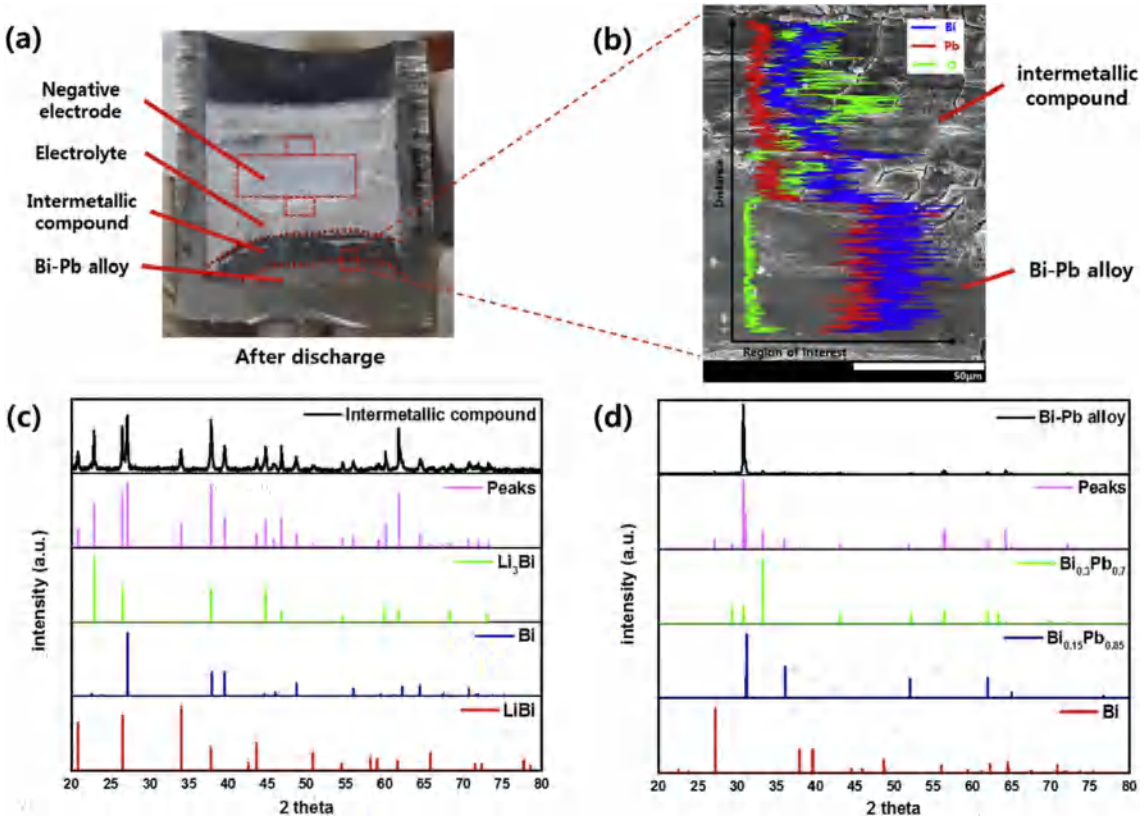

Fig. 3. (a) Cross sectional image of Li|LiCl-LiI|Bi-Pb cell after Li negative electrode was removed. (b) SEM image and EDS mapping at the boundary between the intermetallic compound and Bi-Pb alloy layers. XRD patterns of positive electrode at the discharging state for the (c) intermetallic compound part and (d) Bi-Pb alloy part.

oxygen [10]. The oxygen elemental distribution is only observed in the intermetallic compound region, and not detected in the Bi-Pb alloy layer. Although the Bi is observed in both the intermetallic compound and Bi-Pb alloy layers, the Pb is dominantly located in the Bi-Pb alloy layer. This result indicates that Li selectively reacts with Bi in Bi-Pb alloy. Fig. 3c and d exhibit the XRD patterns of intermetallic compound and Bi-Pb alloy layers respectively. The Li_3Bi, LiBi and Bi phases were observed in the intermetallic compound layer. On the other hand, the phases of $Bi_{0.3}Pb_{0.7}$ (ε-phase) and $Bi_{0.15}Pb_{0.85}$ alloys were observed in the Bi-Pb alloy layer. The Bi-Pb eutectic alloy (Bi:Pb = 55:45 mol %) was decomposed into two phases of Li_xBi and Bi-Pb alloy by discharge process as Li primarily reacts with Bi phase in Bi-Pb eutectic alloy correlating with EDS results and the XRD pattern of the Bi-Pb eutectic alloy. The XRD pattern of the Bi-Pb eutectic alloy shows the Bi phase and ε-phase even after 500th cycles (Figure S6). From the electromotive force (EMF) measurements, the activity of Li is related to EMF by following equation [25].

$$a_{Li} = \exp\left\{\frac{FE}{RT}\right\}$$

Where a_{Li} is activity of Li in the Li-Bi or Li-Pb alloy, F the faraday constant, R the gas constant, T the liquid temperature and E is the EMF value. Through the previous studies about EMF of Bi and Pb with Li content [13,26], Bi has the higher activity with Li compared to Pb. This result indicates that Li primarily reacts with Bi electrochemically [10,11]. Hence, the Pb in the Li|LiCl-LiI|Bi-Pb cell plays a role in the engineering of the physical properties of positive electrode material, such as 1) decreasing the melting temperature and 2) improving the wettability with current collector.

The Li|LiCl-LiI|Bi-Pb cell was operated at optimized temperature, 410 °C. The Ohmic resistance of the cell significantly is decreased at 410 °C through the results of electrochemical impedance spectroscopy (EIS). The Ohmic resistance is not more decreased since the electrolyte is liquefied and stabilized into three distinct layers (Figure S7). Fig. 4a and b shows the initial charge-discharge voltage profile and voltage profiles with different current densities for the cell with a nominal capacity of 1.5 Ah, respectively. During the discharging, the cell exhibits a voltage slope up to 0.62 V, corresponding to the formation of Li_xBi (l) phase, the voltage plateau at 0.62 V, attributed to the coexistence of Li_xBi (l) and Li_3Bi (s) phases. On the other hand, the cell exhibits a long voltage plateau at 0.84 V. The cell shows high initial Coulombic efficiency of 99.4% supporting the high reversibility of the Li||LiCl-LiI||Bi-Pb cell. And it has an energy density of about 86 Wh/kg at 100 mA cm^{-2}, which is almost 88% lower than that of the Li|LiF-LiCl-LiI|Sb-Pb cell at the same current density. However, our system has much lower operation temperature (410 °C) compared to Li|LiF-LiCl-LiI|Sb-Pb cell (450 °C), which enables the reduction of the operation cost (Table S2) [11].

The cycle performance of the Li|LiCl-LiI|Bi-Pb cell with a nominal capacity of 1 Ah was carefully monitored for 1000th cycles (Fig. 4c). Although initial capacity of cell is unstable due to the irreversible reaction caused by the residual moisture and oxygen inside the cell and the interface stabilization between the electrode materials and electrolyte, it exhibits good capacity retention of 86.5% and high Coulombic efficiency over 99.3% during 1000th cycles. The cell was cooled down to room temperature at 479th cycle, and the cycle performance was evaluated after re-heating to 410 °C. Even after the thermal variation, the cell shows stable cycle performance with high Coulombic efficiencies and a low Ohmic resistance during further cycling (Figure S7). High stability of the Li|LiCl-LiI|Bi-Pb cell is revealed by analysis of DSC, XRD, SEM, and EDS. Even after long cycles, physical properties of cell are no noticeable difference although some effects of oxidation (Figure S4b, S6, S8). Fig. 4d shows the voltage profiles at different cycle numbers. Even after long cycles and thermal variation, the cell shows stable voltage profiles without noticeable polarizations. The electrochemical properties of the Li|LiCl-LiI|Bi-Pb cell clearly support that our

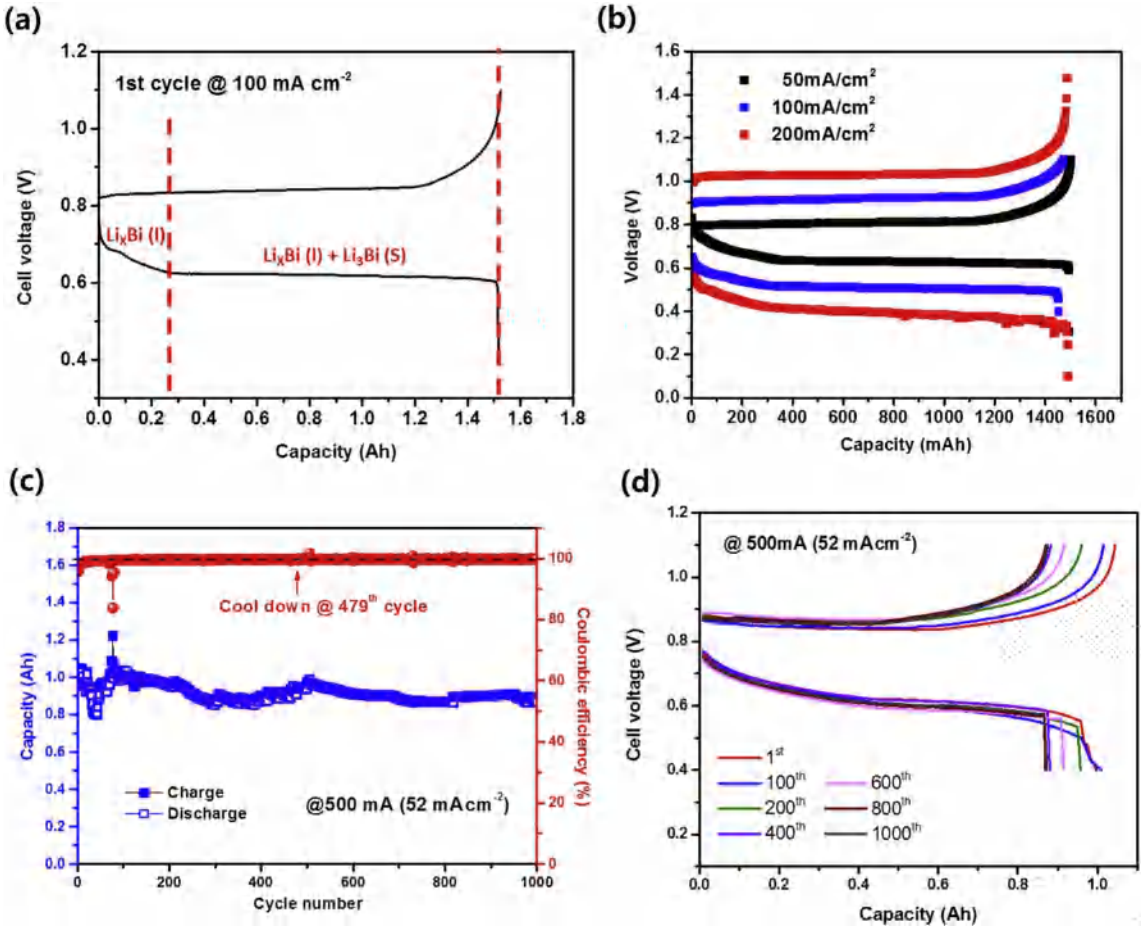

Fig. 4. Electrochemical characterization of Li|LiCl-LiI|Bi-Pb cell in the voltage range between 0.4 and 1.1 V. Voltage profiles of the cell with 1.5 Ah capacity (a) at the first cycle and (b) at different current densities; Cycle performance of the cell with 1 Ah capacity at the current density of 52 mA cm^{-2}. (c) Charge and discharge capacity and corresponding Coulombic efficiency. (d) Voltage profiles at different cycle number.

designed molten salt electrolyte and alloy positive electrode are suitable for LMBs operating at low temperature to minimize the maintenance cost and address corrosion issue in the cell.

4. Conclusions

In summary, we investigated the electrochemical properties of Li|LiCl-LiI|Bi-Pb cell, in which a molten salt electrolyte of LiCl-LiI (LiCl:LiI = 36:64 mol %) and a positive electrode of Bi-Pb eutectic alloy (Bi:Pb = 55.5:44.5 mol %) were employed to lower the cell operation temperature. The molten salt electrolyte has a low melting temperature of 370 °C and low self-discharge values (< 0.05 mA cm^{-2}). The alloying Bi with Pb decreases its melting temperature and improves the wettability on the SUS304 current collector. The Li|LiCl-LiI|Bi-Pb cell with 1Ah capacity exhibits stable cycle performance of 86.5% and high Coulombic efficiencies over 99.3% during 1000^{th} cycle at 410 °C. Even after the thermal variation, the cell shows reversible electrochemical properties. These results demonstrate that the LiCl-LiI molten salt electrolyte and Bi-Pb eutectic alloy positive electrode could be promising components to achieve LMBs with robust electrochemical properties.

Acknowledgements

This work was supported by the Energy Efficiency & Resources Core Technology Program of the Korea Institute of Energy Technology Evaluation and Planning (KETEP) granted financial resource from the Ministry of Trade, Industry & Energy, Republic of Korea (No. 20142020104190) and the 2015 Research Fund (1.150034.01) of UNIST (Ulsan National Institute of Science and Technology).

Appendix A. Supplementary data

Supplementary data related to this article can be found at http://dx.doi.org/10.1016/j.jpowsour.2017.11.081.

References

[1] B. Dunn, H. Kamath, J.-M. Tarascon, Science 334 (2011) 928–935.
[2] Z. Yang, J. Zhang, M.C. Kintner-Meyer, X. Lu, D. Choi, J.P. Lemmon, J. Liu, Chem. Rev. 111 (2011) 3577–3613.
[3] T. Oshima, M. Kajita, A. Okuno, Int. J. Appl. Ceram. Technol. 1 (2004) 269–276.
[4] C.-H. Dustmann, J. Power Sources 127 (2004) 85–92.
[5] D. Shin, H. Park, U. Paik, Electrochem. Commun. 77 (2017) 103–106.
[6] R. Wills, J. Collins, D. Stratton-Campbell, C. Low, D. Pletcher, F.C. Walsh, J. Appl. Electrochem. 40 (2010) 955–965.
[7] H. Kim, D.A. Boysen, J.M. Newhouse, B.L. Spatocco, B. Chung, P.J. Burke, D.J. Bradwell, K. Jiang, A.A. Tomaszowska, K. Wang, Chem. Rev. 113 (2012) 2075–2099.
[8] H. Li, H. Yin, K. Wang, S. Cheng, K. Jiang, D.R. Sadoway, Adv. Energy Mater. 6 (2016).
[9] X. Ning, S. Phadke, B. Chung, H. Yin, P. Burke, D.R. Sadoway, J. Power Sources 275 (2015) 370–376.
[10] H. Li, K. Wang, S. Cheng, K. Jiang, ACS Appl. Mater. interfaces 8 (2016) 12830–12835.
[11] K. Wang, K. Jiang, B. Chung, T. Ouchi, P.J. Burke, D.A. Boysen, D.J. Bradwell, H. Kim, U. Muecke, D.R. Sadoway, Nature 514 (2014) 348–350.
[12] B.L. Spatocco, T. Ouchi, G. Lambotte, P.J. Burke, D.R. Sadoway, J. Electrochem. Soc. 162 (2015) A2729–A2736.
[13] W. Weppner, R. Huggins, J. Electrochem. Soc. 125 (1978) 7–14.
[14] C.E. Johnson, E.J. Hathaway, J. Chem. Eng. Data 14 (1969) 174–175.

[15] D.J. Bradwell, H. Kim, A.H. Sirk, D.R. Sadoway, J. Am. Chem. Soc. 134 (2012) 1895–1897.
[16] N. Hiramatsu, Y. Uematsu, T. Tanaka, M. Kinugasa, Mater. Sci. Eng. A 120 (1989) 319–328.
[17] H. Asteman, J.-E. Svensson, L.-G. Johansson, M. Norell, Oxid. Metals 52 (1999) 95–111.
[18] R. Patterson, R. Schlager, D. Olson, J. Nucl. Mater. 57 (1975) 312–316.
[19] X. Lu, G. Li, J.Y. Kim, J.P. Lemmon, V.L. Sprenkle, Z. Yang, J. Power Sources 215 (2012) 288–295.
[20] R. Novakovic, E. Ricci, D. Giuranno, F. Gnecco, Surf. Sci. 515 (2002) 377–389.
[21] Y. Plevachuk, V. Sklyarchuk, G. Gerbeth, S. Eckert, R. Novakovic, Surf. Sci. 605 (2011) 1034–1042.
[22] D. Giuranno, F. Gnecco, E. Ricci, R. Novakovic, Intermetallics 11 (2003) 1313–1317.
[23] A.V. Virkar, L. Viswanathan, D.R. Biswas, J. Mater. Sci. 15 (1980) 302–308.
[24] N. Gokcen, J. Phase Equilibria 13 (1992) 21–32.
[25] M.M. Kane, J.M. Newhouse, D.R. Sadoway, J. Electrochem. Soc. 162 (2015) A421–A425.
[26] W. Gasior, Z. Moser, J. Nucl. Mater. 294 (2001) 77–83.